Int. J. Electrochem. Sci., 4 **(2009)** 77 - 103

International Journal of ELECTROCHEMICAL SCIENCE
www.electrochemsci.org

Transport and Kinetics at Carbon Nanotube – Redox Enzyme Composite modified Electrode Biosensors

Michael E.G. Lyons[*]

Physical and Materials Electrochemistry Laboratory, School of Chemistry, University of Dublin, Trinity College, Dublin 2, Ireland.
[*]E-mail: melyons@tcd.ie

Received: 28 October 2008 / *Accepted:* 15 November 2008 / *Published:* 20 December 2008

A mathematical model describing transport and kinetics of substrate and redox mediator within chemically modified electrodes comprising of redox enzymes immobilized in dispersed carbon nanotube meshes dispersed on support electrode surfaces is described. Two modes of amperometric detection are subjected to analysis. In the first the current arising from re-oxidation of the reduced mediator at the support electrode is measured, whereas in the second the current arising from reduction of the oxidized mediator at the support surface is determined. Approximate analytical expressions for the substrate reaction flux within the nanotube layer are developed and related to the measured flux at the support surface. The kinetics both of substrate and mediator within the layer are also represented in terms of a kinetic case diagram.

Keywords: Amperometric enzyme biosensor modeling; Single wall/ redox enzyme composite; SWNT modified electrodes. Immobilized redox enzyme systems.

1. INTRODUCTION

The science of the 21st century will be driven by the direct manipulation of events at the atomic or molecular level. More generally, the nanoscale is where new and unexpected discoveries, of potential technical value, will be made [1]. Investigating and manipulating the nanoscale will in many ways define the science and technology of the 21st century. Since the discovery by Iijima [2] in 1993, carbon nanotubes have attracted enormous international interest because of their unique structural, mechanical and electronic properties. The electrochemical properties of both multi (MWCNT) and single walled (SWCNT) carbon nanotubes are only now being subjected to intensive examination due largely to the fact that these materials should serve as excellent candidates for nanoelectrodes and platforms for nanoelectrochemical cells and amperometric biosensor devices [3-5].

Electron transfer in biological systems is one of the leading areas in the biochemical and biophysical sciences [6], and in recent years there has been considerable interest in the direct electron transfer between redox proteins and electrode surfaces [7]. However in the absence of mediating small molecules, the observation of well defined electrochemical behaviour of immobilized flavoprotein oxidase systems such as Glucose Oxidase (GOx) is rendered extremely difficult, because the FAD group is embedded deep within the protein structure thereby making the transmission coefficient for direct electron transfer between the latter and a support electrode very small [8]. Various immobilization strategies [9,10] have been adopted to fabricate enzyme electrodes for biosensor applications. These strategies have exhibited variable degrees of success and in many cases electron transfer mediators have been used to facilitate electronic communication between the active site of the protein and the underlying electrode. However the potential at which an amperometric enzyme biosensor is operated depends on the redox potential of the mediator used rather than that exhibited by the active site of the redox enzyme. Usually the difference in magnitude between the latter potentials is significant (ca. 0.3-0.5V) and is a factor which acts against successful biosensor operation, since the more positive the operating potential, the greater is the tendency for the sensor to respond to oxidizable substances present in ther sample other than the target substrate. Clearly the best strategy for successful enzyme biosensor fabrication is to devise a configuration by which electrons can directly transfer from the redox center of the enzyme to the underlying support electrode. This has been accomplished in recent years using the concept of molecular wiring.

The similarity in length scales between carbon nanotubes and redox enzymes suggest the presence of interactions that may be favourable for biosensor application [11]. The strategy of physical adsorption or covalent immobilization of large biomolecules onto the surface of immobilized carbon nanotubes may well represent an exciting pathway through which direct electrical communication between support electrodes and the active site of redox enzymes can be achieved. For instance recent work [12,13] has indicated that the chemical modification of electrode surfaces with carbon nanotubes has enhanced the activity of the latter with respect to the reaction of biologically active species such as hydrogen peroxide, dopamine and NADH. Furthermore multi-walled carbon nanotubes have been shown to exhibit good electronic communication with redox proteins where not only the redox center is close to the proteins surface such as found with cytochrome c, azurin and horseradish peroxidase, but also when it is embedded deep with the glycoprotein sheath such as is found with glucose oxidase [14,15]. In the present paper we report on the well resolved redox behaviour and excellent catalytic properties of glucose oxidase adsorbed on the surface of single wall carbon nanotubes which have been dispersed on the surface of support electrodes to form a random mesh of high surface area.

In the present paper we develop a theoretical model which describes transport and kinetics at electrodes which have been chemically modified with highly dispersed meshes of single wall carbon nanotubes on which redox enzymes such as glucoes oxidase have been adsorbed. The latter composite has recently been shown [16] to exhibit excellent activity as an electrochemical enzyme electrode for the amperometric detection of glucose at very low potential. We have also recently indicated that the redox properties of the flavin groups located within the immobilized enzyme may be directly probed and quantified using electrochemical techniques such as cyclic voltammetry and potential step chronoamperometry [17,18].

We focus attention on understanding the catalytic behaviour of a redox enzyme such as glucose oxidase (GOx) adsorbed on the sidewall of a single wall carbon nanotube. The latter is assumed to form a highly dispersed mesh on a support electrode thereby enabling a high loading of enzyme to be obtained which is located in close proximity to the electrode surface. In our previous experiments we have used cyclic voltammetry to show that the surface coverage of adsorbed GOx lies in the range 90-160 pmol cm^{-2} [18]. Hence the loading of redox enzyme will be relatively high. We have also shown in our previous work [16] that a soluble redox mediator such as molecular oxygen or ferrocene monocarboxylic acid is required when the SWCNT.GOx composite is used as an amperometric electrode. Hence the mathematical model will consider both the transport of substrate and mediator in the solution to the electrode surface, the enzyme/mediator and enzyme substrate reaction kinetics and the reaction kinetics of the mediator at the support electrode surface. Furthermore the detailed relationship between the substrate reaction flux f_S and the observed flux f_Σ measured at the electrode is determined.

2. THEORETICAL MODEL

2.1. General considerations

A schematic representation of the SWCNT mesh modified electrode in which GOx molecules are distributed is illustrated in figure 1.

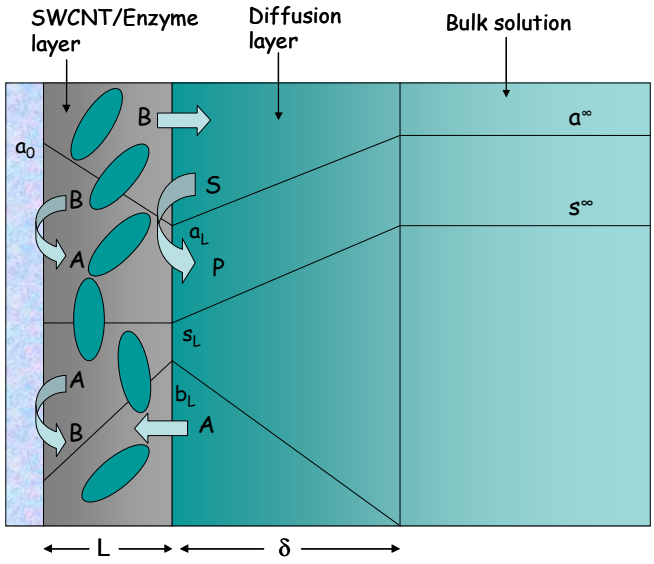

Figure 1. Schematic representation of immobilized enzyme electrode using a soluble redox mediator. The concentration polarization of substrate within the enzyme layer is neglected but a Nernst diffusion layer treatment for substrate and mediator transport in the solution is adopted.

The reaction scheme is based on a redox enzyme such as Glucose Oxidase which follows a 'ping-pong' reaction mechanism. In the figure A/B represents the mediator redox couple. In our

system A denotes O_2 and B represents H_2O_2. Hence A denotes the oxidised form of the mediator and B represents the reduced form. Furthermore E_O and E_R represent the oxidized and reduced forms of the enzyme and S,P denote the substrate and product (glucose and gluconolactone) respectively. We also assume that the enzyme is immobilized in a homogeneous manner within the SWCNT matrix which has a thickness L. We also assume that the SWCNT mesh immobilized on the electrode surface (typically a gold or glassy carbon electrode) is very open and porous and so we can neglect concentration polarization of both substrate and redox mediator within the enzyme layer. We only consider diffusion of the latter within the solution adjacent to the modified electrode and use the Nernst diffusion layer approximation to describe the latter process. The substrate is free to diffuse through the film with a diffusion coefficient D_S . It should be noted that the diffusion coefficient for transport within the nanotube layer may differ in magnitude from that exhibited by the substrate in the solution adjacent to the layer. The latter process is quantified by the paramerer D'_S . Partitioning of the substrate across the layer/solution interface occurs and is quantified by a substrate partition coefficient κ_S. The oxidized form of the mediator (O_2) is present in the bulk solution at a concentration a^{∞} whereas it is assumed that the concentration of the reduced form of the mediator (H_2O_2) is zero in the bulk solution outside the Nernst diffusion layer which is assumed to have a thickness δ. The partition coefficient of the mediator is designated κ_A.

We consider the following reaction sequence presented in scheme 1. In this reaction sequence within the SWCNT layer the oxidised form of the enzyme E_O reacts with the substrate S to form product P and reduced enzyme E_R. This process occurs via Michaelis-Menten kinetics with characteristic parameters Michaelis constant K_M and catalytic rate constant k_c.

Layer

$$S + E_O \underset{}{\overset{K_M}{\rightleftarrows}} E_O S \xrightarrow{k_c} E_R + P$$

$$E_R + A \underset{}{\overset{K'_M}{\rightleftarrows}} E_R A \xrightarrow{k} E_O + B$$

Electrode

$$B \xrightarrow{k'} A$$

or

$$A \xrightarrow{k'} B$$

Scheme 1 Summary of kinetics within nanotube layer and at electrode surface

Furthermore it is assumed that the oxidised form of the mediator partitions into the nanotube layer, diffuses within it and reacts with the reduced enzyme (again most generally via a Michaelis Menten mechanism) to regenerate the catalytically active oxidized enzyme. The latter process is defined by parameters K'_M ,the mediator Michaelis constant, and k the rate constant for dissociation of mediator-enzyme complex.

2.2. Relating the observed flux to the substrate transformation flux

The enzyme/substrate reaction and the enzyme/mediator reaction are assumed to give rise to a substrate flux f_S which is measured in the usual units of amount transformed per unit area per unit time (mol cm^{-2} s^{-1}). This will be related in some defined manner to the observed flux f_Σ which is measured at the electrode and is related to the current flowing via the expression

$$f_\Sigma = \frac{i}{nFA} \tag{1}$$

where n,F and A denote the number of electrons transferred, the Faraday constant and the electrode geometric area respectively. The exact relationship depends on the mode of amperometric detection used at the support electrode. As indicated in scheme 1 and in more detail in schemes 2 and 3, two possibilities arise.

The first and more usual mode is that the reduced mediator diffuses to the support electrode where it is reoxidized. This is characterized by a heterogeneous electrochemical rate constant k'. In this scenario the measured flux will be proportional to the substrate concentration as is usual in analytical chemistry. This idea is illustrated in scheme 2. This detection mode suffers from the disadvantage that reoxidation of the reduced mediator may well require a significantly positive potential thereby reducing the selectivity of the detection method.

Alternatively, as presented in scheme 3 below, the oxidized mediator A will be detected at the support electrode where it will be reduced to B. Only a fraction of the available A molecules will be available for direct reaction at the electrode (the kinetics of the latter being again described by the heterogeneous rate constant k') since some portion will also react with the reduced enzyme . Hence a competition exists for the services of the oxidized mediator between a direct reaction at the support electrode surface and reaction with reduced enzyme. Hence in this latter situation the measured flux in the presence of substrate will be *less* than that measured in the absence of substrate and the *flux difference* will be proportional to substrate concentration when the detection conditions are such that saturation of enzyme by substrate will pertain. This detection method is very attractive since it may occur at quite a low potential where very few interferent species may simultaneously react.

We assume that the heterogeneous rate constant k' is well described by the Butler-Volmer equation:

$$k' = k^0 \exp\left[\pm\frac{\beta F \xi}{RT}\right] = k^0 \exp\left[\pm\frac{\beta F\left(E - E^0\right)}{RT}\right] \tag{2}$$

where ξ denotes a normalised potential , β is the symmetry factor (typically ½) and the other symbols have their usual meanings (all symbols are defined in the glossary at the end of the paper). When the heterogeneous electrochemical rate constant is very large then the mediator concentrations at the layer/electrode interface will be related via the well established Nernst equation.

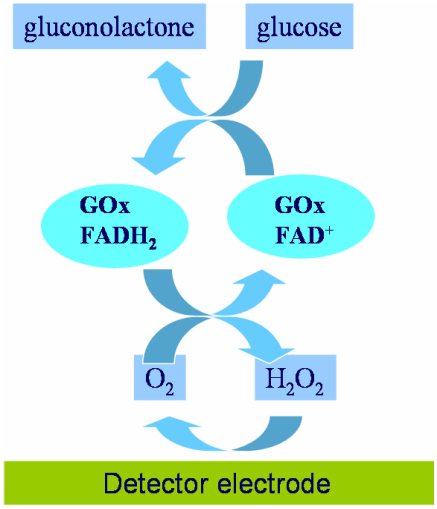

Scheme 2 Traditional amperometric detection strategy at SWCNT/enzyme electrode.

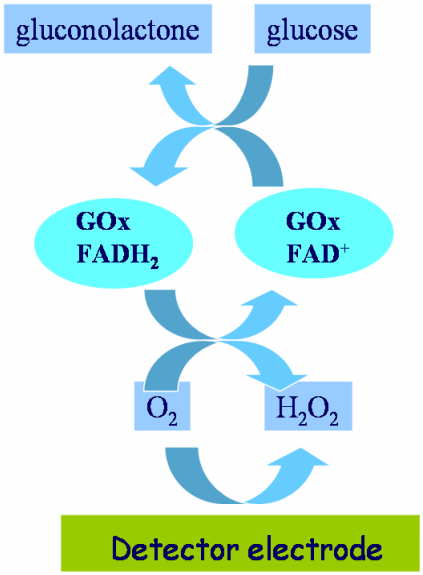

Scheme3 Mediator 'competition' strategy for low potential amperometric detection at SWCNT /enzyme electrode

We can relate the amperometric current to the mediator flux at the electrode surface via the following relationship

$$f_{\Sigma} = D_B \left(\frac{db}{dx} \right)_{x=0}$$
$$f_{\Sigma} = D_A \left(\frac{da}{dx} \right)_{x=0} \qquad (3)$$

The first of the expressions in eqn.3 refers to the situation where the reduced mediator is re-oxidized at the electrode whereas the second refers to the case where the oxidized mediator is reduced at the electrode.

We must realise that the flux of substrate reacting within the nanotube film (the substrate flux) is not necessarily the same as the flux of reduced mediator detected at the support electrode [19,20]. In appendix A we will show that for the situation where the oxidation of reduced mediator B is detected at the electrode, the measured flux f_Σ is related to the substrate reaction flux f_S via the following expression

$$f_\Sigma = \eta f_S \tag{4}$$

where the η parameter is given by

$$\eta = \frac{1+\frac{\theta}{2}}{1+\theta(1+\phi)} \tag{5}$$

where we have defined

$$\begin{aligned} \theta &= \frac{D_B'/\delta}{\kappa_B D_B/L} = \frac{k_D'}{k_D} \\ \phi &= \frac{\kappa_B D_B/L}{\kappa_B k'} = \frac{k_D}{\kappa_B k'} \end{aligned} \tag{6}$$

Hence θ defines the balance between reduced mediator transport in the diffusion layer defined by the diffusive rate parameter k'_D and reduced mediator transport in the SWCNT layer defined by the diffusive rate parameter k_D . Furthermore φ relates the balance between the diffusive transport of reduced mediator in the layer to the heterogeneous reaction of the reduced mediator at the support electrode surface. It is gratifying to note that the heterogeneous rate constant k' is modified by the partition coefficient of the reduced mediator κ_B. Clearly φ will depend on the magnitude of the electrode potential. When the potential E applied to the detector electrode is very large k' will be large and so $\kappa_B k' >> k_D$ and $\phi \to 0$ and from eqn.5 we note that

$$\eta \cong \frac{1+\frac{\theta}{2}}{1+\theta} \tag{7}$$

The variation of η with θ according to eqn.7 is presented in fig.2. We note that when $\theta << 1$ corresponding to the case where diffusion in the solution is much slower than diffusion in the layer, there will be much reduced mediator present in the layer and $\eta \to 1$ and $f_\Sigma \cong f_S$. Conversely, when $\theta >> 1$, the reduced mediator B will be lost rapidly from the layer into the adjacent solution, there will be

correspondingly less reduced mediator present for reaction at the support electrode and so the observed flux will be less than the substrate reaction flux with $\eta \cong 1/2$. Hence to a good approximation when the kinetics of reduced mediator oxidation at the electrode are rapid $0.5 \le \eta \le 1$.

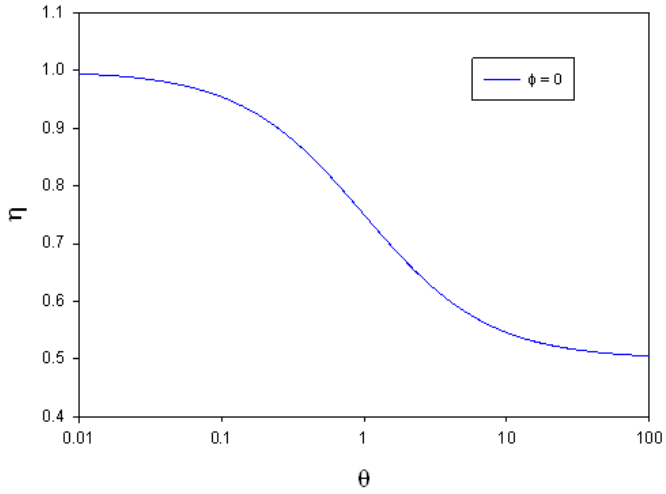

Figure 2. Variation of the flux efficiency factor η with the mediator diffusive flux ratio θ

The situation is more complicated when the alternative mode of detection is employed where the oxidized mediator is reduced at low potential at the support electrode surface in direct competition with its reaction with the reduced enzyme. This situation is described in detail in appendix B. There we show that the difference between the flux measured in the absence of substrate and that measured in the presence of substrate is related to the substrate reaction flux via

$$\Delta f_{\Sigma} = f_{\Sigma,0} - f_{\Sigma} = \eta' f_S \tag{8}$$

where we define

$$\eta' = \frac{1+\frac{f'_D}{2f_D}}{1+\frac{f'_D}{f_K}+\frac{f'_D}{f_D}} = \frac{1+\frac{\theta}{2}}{1+\theta+\varepsilon} \tag{9}$$

In the latter expression the parameter ε defines the balance between the diffusive flux of oxidized mediator in solution and the kinetic flux for oxidized mediator resuction at the support electrode. When the electrode kinetics are rapid then $f_K = \kappa_A k' a^{\infty}$ is large and consequently $\varepsilon = f'_D / f_K << 1$ and as noted in appendix B, the theoretical approach underlying eqn.8 breaks down.

2.3. Determination of the substrate reaction flux within the SWCNT/enzyme layer

As previously noted the immobilized nanotube layer is thin we so we can neglect diffusion of substrate within the film. Furthermore we can neglect enzyme diffusion since the latter is immobilized

on the dispersed nanotube mesh. If substrate diffusion is specifically considered then the analysis of Bartlett and Whitaker [21] , Marchesiello and Genies [22] and Bartlett and Pratt [23] pertain. This area has been summarised by Lyons [24], and more recently by Bartlett and Calvo [25].

Hence we need to consider the rates of two processes : the reaction between oxidized enzyme and substrate and the reaction between reduced enzyme and oxidised mediator. The first process depletes the catalytically active enzyme whereas the second replenishes it. We assume that both reactions are well described by a Michaelis-Menten kinetic scheme, and we write:

$$\begin{aligned} E_O + S &\xrightarrow{k_E} E_R + P \\ A + E_R &\xrightarrow{k_M} B + E_O \end{aligned} \tag{10}$$

where the rate constants k_E and k_M are given by:

$$\begin{aligned} k_E &= \frac{k_c}{K_M + s} \\ k_M &= \frac{k}{K'_M + a} \end{aligned} \tag{11}$$

In the latter expressions s and a represent the substrate and oxidized mediator concentrations within the nanotube film.

At steady state the mediator/nzyme flux and enzyme/substrate must be in balance and the substrate reaction flux f_S is given by

$$f_S = \frac{k_c e_O \kappa_S s_L L}{K_M + \kappa_S s_L} = \frac{k \kappa_A a_L e_R L}{K'_M + \kappa_A a_L} \tag{12}$$

where we have assumed that $a = \kappa_A a_L$ and $s = \kappa_S s_L$ where a_L and s_L represent the oxidized mediator and substrate concentrations at the outer edge of the nanotube layer at x = L. We note that e_O and e_R denote the concentrations of oxidized and reduced enzyme respectively. If e_Σ represents the total enzyme concentration in the nanotube layer then $e_\Sigma = e_O + e_R$ .Here we have neglected the concentrations of the bound enzyme since they area very small. Rearrangement of the flux expression in eqn.12 in terms of total enzyme concentration results in:

$$f_S = \frac{k_c \kappa_S s_L k \kappa_A a_L e_\Sigma L}{k_c \kappa_S s_L \left(\kappa_A a_L + K'_M\right) + k \kappa_A a_L \left(\kappa_S s_L + K_M\right)} \tag{13}$$

We now take the effect of substrate and mediator concentration polarization in solution into account. We do this by matching the substrate reaction flux in the layer with the substrate and mediator diffusive fluxes in the solution. In the context of the Nernst diffusion layer approximation [26] we note

$$f_S = D'_S\left(\frac{s^\infty - s_L}{\delta}\right) = k'_{DS}\left(s^\infty - s_L\right)$$
$$= D'_A\left(\frac{a^\infty - a_L}{\delta}\right) = k'_{DA}\left(a^\infty - a_L\right) \quad (14)$$

and so we obtain on further simplification:

$$s_L = s^\infty - \frac{f_S}{k'_{DS}} = s^\infty\left(1 - \frac{f_S}{f'_{DS}}\right) = s^\infty T_S$$
$$a_L = a^\infty - \frac{f_S}{k'_{DA}} = a^\infty\left(1 - \frac{f_S}{f'_{DA}}\right) = a^\infty T_A \quad (15)$$

where $f'_{DS} = k'_{DS}s^\infty$ and $f'_{DA} = k'_{DA}a^\infty$ represent the diffusive fluxes of substrate and oxidized mediator in the solution adjacent to the nanotube film. We note from eqn.14 that the effects of concentration polarization will be important when the net reaction flux f_S becomes close to the limit imposed by the diffusive transport of substrate through the solution given by $f'_{DS} = k'_{DS}s^\infty$. Under these circumstances the substrate concentration within the layer at x = L will differ appreciably from the value in the bulk solution and the enzyme will be less saturated than one would expect from the value of the bulk concentration. A similar consideration pertains for the oxidized mediator species concentration a_L at the layer/solution interface [27-29].

Substituting the results obtained in eqn.15 into the flux expression presented in eqn.13 we obtain:

$$f_S = \frac{k_c\kappa_S s^\infty T_S k\kappa_A a^\infty T_A e_\Sigma L}{k_c\kappa_S s^\infty T_S\left(\kappa_A a^\infty T_A + K'_M\right) + k\kappa_A a^\infty T_A\left(\kappa_S s^\infty T_S + K_M\right)} \quad (16)$$

We can readily simplify this rather complex expression by inverting both sides to obtain:

$$\frac{1}{f_S} = \frac{1}{\left(k/K'_M\right)T_A\kappa_A a^\infty e_\Sigma L} + \frac{1}{\left(k_c/K_M\right)T_S\kappa_S s^\infty e_\Sigma L} + \frac{1}{ke_\Sigma L} + \frac{1}{k_c e_\Sigma L} \quad (17)$$

The first term on the rhs of eqn.17 corresponds to rate determining unsaturated oxidized mediator/reduced enzyme reaction kinetics modified by a mediator transport term T_A, the latter defined in eqn.15. The unsaturated bimolecular rate constant is $k'_U = k/K'_M$. The second term corresponds to rate determining unsaturated oxidized enzyme/substrate reaction kinetics quantified by a bimolecular rate constant $k_U = k_c/K_M$. Again this term is modified by the transport term T_S defined in eqn.15. The third term describes saturated enzyme kinetics involving rate determining decomposition of the enzyme/substrate complex and the fourth and final term in eqn.17 corresponds to rate determining saturated kinetics involving decomposition of the redox mediator/ enzyme complex.

If $f_S/f'_{DS} << 1$ and $f_S/f'_{DA} << 1$ then we can neglect concentration polarization and $T_A \to 1$ $T_S \to 1$ and eqn.16 reduces to:

$$f_S = \frac{k_c \kappa_S s^\infty k \kappa_A a^\infty e_\Sigma L}{k_c \kappa_S s^\infty \left(\kappa_A a^\infty + K'_M\right) + k \kappa_A a^\infty \left(\kappa_S s^\infty + K_M\right)} \tag{18}$$

whereas eqn.17 is given by:

$$\frac{1}{f_S} = \frac{1}{\left(k/K'_M\right)\kappa_A a^\infty e_\Sigma L} + \frac{1}{\left(k_c/K_M\right)\kappa_S s^\infty e_\Sigma L} + \frac{1}{k e_\Sigma L} + \frac{1}{k_c e_\Sigma L} \tag{19}$$

We note that eqn.18 is a representation of the general Michaelis Menten rate equation for the Ping-Pong mechanism whereas eqn.19 is the corresponding representation of the generalised Lineweaver-Burk equation [25].

2.4. Problem definition in terms of dimensionless variables and kinetic case diagrams

We now follow the procedure adopted in our previous papers and develop a kinetic case diagram for an immobilized enzyme electrode system. We assume that the SWNT layer is thin . In this analysis we also neglect concentration polarization of mediator and substrate in solution . We will assume that both the mediator/enzyme reaction and the substrate/enzyme reaction are described by Michaelis-Menten kinetics. Under such circumstances the reaction flux is given by eqn.17 . We can introduce a normalised substrate flux as,

$$\Psi_S = \frac{f_S}{f_{S,\max}} = \frac{f_S}{k_C e_\Sigma L} \tag{20}$$

where $f_{S,\max}$ denotes the maximum enzyme turnover rate. We also introduce saturation parameters α and β for substrate and mediator as follows,

$$\begin{aligned} \alpha &= \frac{\kappa_S s^\infty}{K_M} \\ \beta &= \frac{\kappa_A a^\infty}{K'_M} \end{aligned} \tag{21}$$

We finally introduce a kinetic competition parameter γ as follows

$$\gamma = \frac{\left(k/K'_M\right)\kappa_A a^\infty}{\left(k_C/K_M\right)\kappa_S s^\infty} = \frac{k'_U \kappa_A a^\infty e_\Sigma L}{k_U \kappa_S s^\infty e_\Sigma L} = \frac{f_{ME}}{f_{SE}} \tag{22}$$

Hence γ compares the mediator/enzyme reaction flux to the substrate/enzyme reaction flux. When γ << 1 then $f_{ME} << f_{SE}$ and the net flux is limited by the kinetics of the bimolecular reaction between mediator and enzyme. In contrast when γ >> 1 then $f_{ME} >> f_{SE}$ and the net flux is limited by

the kinetics of the reaction between substrate and enzyme. The substrate saturation parameter α compares the value of the substrate concentration in the layer $\kappa_S s^\infty$ to the Michaelis constant K_M for substrate. When $\alpha << 1$ then $\kappa_S s^\infty << K_M$ and we have unsaturated enzyme kinetics. In contrast when $\alpha >> 1$ then $\kappa_S s^\infty >> K_M$, and saturated enzyme kinetics pertain. The mediator saturation parameter β compares the oxidized mediator concentration within the layer, $\kappa_A a^\infty$, to the Michaelis constant for the mediator K'_M. When $\beta << 1$, $\kappa_A a^\infty << K'_M$, and unsaturated mediator kinetics pertain. This is the situation usually considered in the literature. On the other hand when the mediator concentration within the layer is large, then $\kappa_A a^\infty >> K'_M$, saturated mediator kinetics will apply and $\beta >> 1$.

If eqn.20-eqn.22 are introduced into eqn.18 we obtain after some algebra,

$$\Psi_S = \frac{\alpha\gamma}{\gamma(1+\alpha)+1+\beta} \tag{23}$$

This normalised expression for the flux pertains over the entire range of substrate and mediator concentrations. We can simplify the analysis and assume firstly that the concentration of redox mediator within the SWNT film is low. Under these conditions $\beta << 1$ and eqn.23 reduces to:

$$\Psi_S \cong \frac{\alpha\gamma}{1+\gamma(1+\alpha)} \tag{24}$$

Eqn.24 can be reduced further depending on the value adopted by the substrate saturation parameter α. When the substrate concentration in the layer is low $\alpha << 1$ and eqn.24 reduces to:

$$\Psi_S \cong \frac{\alpha\gamma}{1+\gamma} \tag{25}$$

This expression is valid for the situation where the mediator and enzyme kinetics are unsaturated. We can simplify still further by examining suitable limiting values of the competition parameter γ.

Firstly, when $\gamma << 1$, we recall that the substrate reaction flux is limited by reaction between oxidized mediator and reduced enzyme. Here the normalized flux is given by:

$$\Psi_S \cong \alpha\gamma \tag{26}$$

We label this situation as case IA. Transforming eqn.26 into an expression for the substrate flux we get:

$$f_S \cong \frac{k}{K'_M} e_\Sigma L \kappa_A a^\infty = k'_U e_\Sigma L \kappa_A a^\infty \tag{27}$$

Hence when the reaction between oxidized mediator and reduced enzyme is rate determining the flux in the film should exhibit a first order dependence on the bulk concentration of oxidized mediator, provided that the concentration of mediator is not too large. The flux should also be independent of the bulk substrate concentration and exhibit a first order dependence both on enzyme loading and layer thickness.

Secondly,when $\gamma >> 1$ the substrate reaction flux in the layer will be limited by the unsaturated reaction kinetics between oxidized enzyme and substrate. In this case the normalized flux takes the form:

$$\Psi_S \cong \alpha \tag{28}$$

We label this situation case IB. Re-transforming into the usual variables we get:

$$f_S \cong \frac{k_C}{K_M} e_\Sigma L \kappa_S s^\infty = k_U e_\Sigma L \kappa_S s^\infty \tag{29}$$

Hence we note that the reaction flux should be first order with respect to bulk substrate concentration, independent of mediator concentration and first order with respect to enzyme loading and layer thickness. Hence case IA and IB pertain when $\alpha << 1$ and when $\beta << 1$.

We now turn to the situation where $\alpha >> 1$ and $\beta << 1$. Re-examination of eqn.24 indicates that the approximate expression for the normalized flux is now given by:

$$\Psi_S \cong \frac{\alpha \gamma}{1+\alpha \gamma} \tag{30}$$

Again we get two limiting cases depending on the value of the product $\alpha\gamma$. Firstly when $\alpha\gamma << 1$ eqn.30 reduces to:

$$\Psi_S \cong \alpha \gamma \tag{31}$$

This is a result which was obtained previously, and case IA is obtained again. Secondly, when $\alpha\gamma >> 1$ eqn.30 reduces to:

$$\Psi_S \cong 1 \tag{32}$$

We label this case II. Here the reaction flux is given by:

$$f_S \cong k_C e_\Sigma L \tag{33}$$

This specific situation corresponds to rate determining saturated enzyme kinetics. The rate limiting step will involve dissociation of the enzyme substrate complex. Here the flux will be

independent both of bulk substrate and mediator concentrations but will depend linearly on enzyme loading and layer thickness.

We have identified three cases (IA, IB and II) when the mediator concentration in the layer is low. We now turn to the situation when the opposite pertains. In this case the general flux expression presented in eqn.23 reduces to:

$$\Psi_S = \frac{\alpha\gamma}{\gamma(1+\alpha)+\beta} \tag{34}$$

Again we can simplify by taking the small α and large α limits. Firstly, when $\alpha << 1$ we get

$$\Psi_S = \frac{\alpha\gamma}{\gamma+\beta} \tag{35}$$

We now compare the magnitudes of the normalized parameters γ and β. When $\gamma << \beta$ eqn.35 reduces to:

$$\Psi_S = \frac{\alpha\gamma}{\beta} \tag{36}$$

We label this situation case III. Transforming to the usual expression for the flux we obtain:

$$f_S \cong k e_\Sigma L \tag{37}$$

Hence case III corresponds to the case of saturated mediator kinetics in which the decomposition of the mediator/enzyme complex to form reduced mediator and oxidized enzyme is rate determining. Here the flux is independent of bulk mediator concentration and bulk substrate concentration , but depends in a first order manner on enzyme concentration and layer thickness.

On the other hand when $\gamma >> \beta$ we get: $\Psi_S \cong \alpha$, which (c.f. eqn.28) again is case IB. Hence case IB pertains also when $\beta >> 1$ and so holds for the entire range of the β parameter.

Turning again to eqn.34, which holds for the case where the mediator concentration in the layer is high, and considering the case $\alpha >> 1$ we obtain:

$$\Psi_S = \frac{\alpha\gamma}{\alpha\gamma+\beta} \tag{38}$$

Again we can get two possible limits by comparing the magnitudes of $\alpha\gamma$ and β . Firstly when $\alpha\gamma << \beta$ we again get case III and the normalised reaction flux reduces to $\Psi_S = \frac{\alpha\gamma}{\beta}$. Whereas in contrast when $\alpha\gamma >> \beta$ we get $\Psi_S \cong 1$, which (c.f.eqn.32) defines case II. Hence case III is valid when the mediator saturation factor β is large and is valid for the entire range of substrate concentrations or α values. Its region of validity will be determined by the conditions $\gamma << \beta$ and $\alpha\gamma << \beta$. Case II, corresponding to saturated enzyme kinetics, is valid for the entire range of β values , and for large values of α, and subject to the restraints that $\alpha\gamma > \beta$ and $\alpha\gamma > 1$. Hence we have identified three cases

(IB, II, III) for the situation where the mediator concentration in the layer is high and all reduced enzyme is bound by mediator.

These various mechanistic and kinetic possibilities are presented in terms of a kinetic case diagram in figure 3. The natural axes defining the case diagram are log α, log β and log γ. Although we indicate the general form of the three dimensional case diagram in figure 3 it is more instructive to examine two limiting slices of the diagram. The first is a plot of log α versus log γ valid for $\beta << 1$. This is illustrated in the lower right inset in figure 3. We see that case IA is located in a block defined by the line $\alpha\gamma = 1$ and $\gamma = 1$. Case IB is defined by the quadrant bordered by the lines $\gamma = 1$ and $\alpha = 1$. Finally case II is defined in terms of the region bordered by the lines $\alpha\gamma = 1$ and $\alpha = 1$. Cases IA, IB and II are most often found experimentally since the mediator concentration in the enzyme layer will usually be low. The second slice of the case diagram is presented in the upper right hand inset in figure 3. Here case IB is bounded by the lines $\beta = \gamma$ and $\beta = 1$. Case II is defined by the lines $\beta = 1$ and $\beta = \alpha\gamma$. Finally case III is delineated by the lines $\beta = \alpha\gamma$ and $\beta = \gamma$.

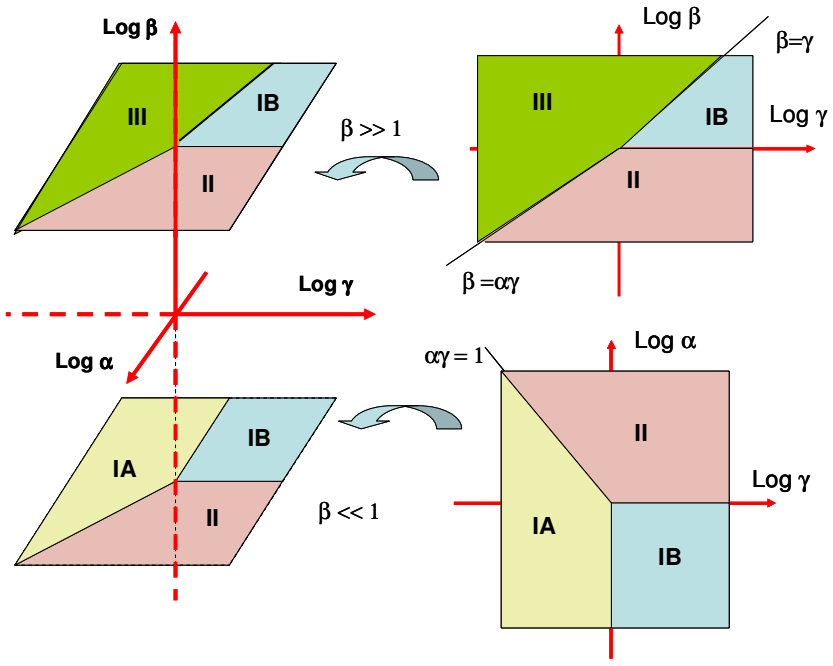

Figure 3. Kinetic case diagram for a SWNT-Enzyme composite film

We summarize the various kinetic possibilities in table 1 where expressions for the normalized flux, and the substrate flux are outlined for the four cases considered. In table 2 we outline the reaction orders with respect to bulk mediator concentration, bulk substrate concentration and enzyme surface coverage $\Gamma_\Sigma = e_\Sigma L$ for each of the rate limiting cases developed in table 1.We note that is is not possible to distinguish between case II and case III by examining the way that the reaction flux varies with enzyme loading, bulk mediator concentration or bulk substrate concentration since an identical set of mechanistic indicators are predicted for both cases.

The variation of normalised reaction flux with substrate saturation parameter is illustrated in fig.4 -fig.6. This is the form in which most experimental batch amperometry data is usually expressed. In this analysis we have indicated the form of the batch amperometry response over a range of mediator concentrations (defined in terms of the mediator saturation parameter β) and for a range of values for the kinetic competition parameter γ which as we have noted defines the balance between the rates of the the oxidized mediator/ reduced enzyme reaction and the substrate/oxidized enzyme reaction flux.

Table 1. Summary of pertinent rate limiting expressions for reaction flux in SWNT-redox enzyme composite modified electrode film.

Kinetic Case	Normalised substrate flux	Substrate flux
IA Unsaturated mediator kinetics	$\Psi_S \cong \alpha\gamma$	$f_S \cong \frac{k}{K'_M} e_\Sigma L \kappa_A a^\infty = k'_U e_\Sigma L \kappa_A a^\infty$
IB Unsaturated enzyme kinetics	$\Psi_S \cong \alpha$	$f_S \cong \frac{k_C}{K_M} e_\Sigma L \kappa_S s^\infty = k_U e_\Sigma L \kappa_S s^\infty$
II Saturated enzyme kinetics	$\Psi_S \cong 1$	$f_S \cong k_C e_\Sigma L$
III Saturated mediator kinetics	$\Psi_S = \frac{\alpha\gamma}{\beta}$	$f_S \cong k e_\Sigma L$

Table 2. Mechanistic indicators for SWNT-immobilized enzyme modified electrodes.

Kinetic case	a^∞	s^∞	Γ_Σ
IA	1	0	1
IB	0	1	1
II	0	0	1
III	0	0	1

In figure 4 the kinetic competition parameter γ is small and set at 0.01, implying that the reaction between oxidized mediator and reduced enzyme is slow and rate limiting. Here the substrate flux does not depend significantly on the substrate concentration as manifested in the substrate saturation parameter α, except when values of the latter is larger than 10. It is interesting to note that

the response to increasing substrate concentration is depressed significantly as the mediator concentration is increased (the latter being represented in terms of the mediator saturation parameter β).

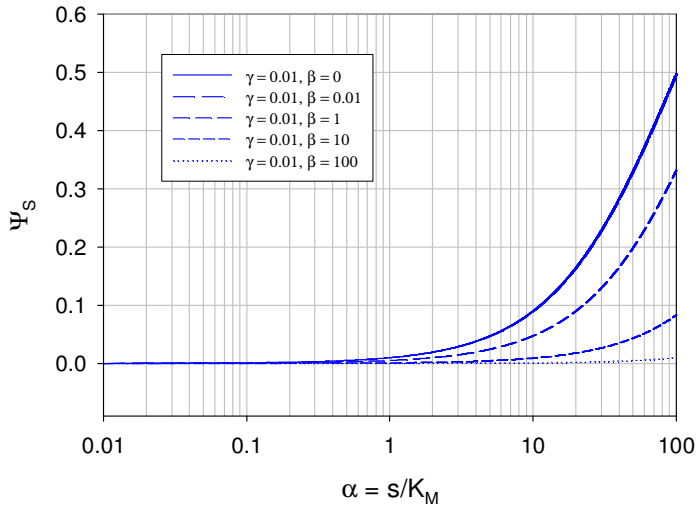

Figure 4. Variation of normalised substrate reaction flux with substrate saturation parameter. The curves are calculated using eqn.23. Here the kinetic competition parameter γ is small and set at 0.01. This implies that the flux for reaction between substrate and oxidized enzyme is much greater than the flux for reaction between oxidized mediator and reduced enzyme and so the latter reaction is rate determining.

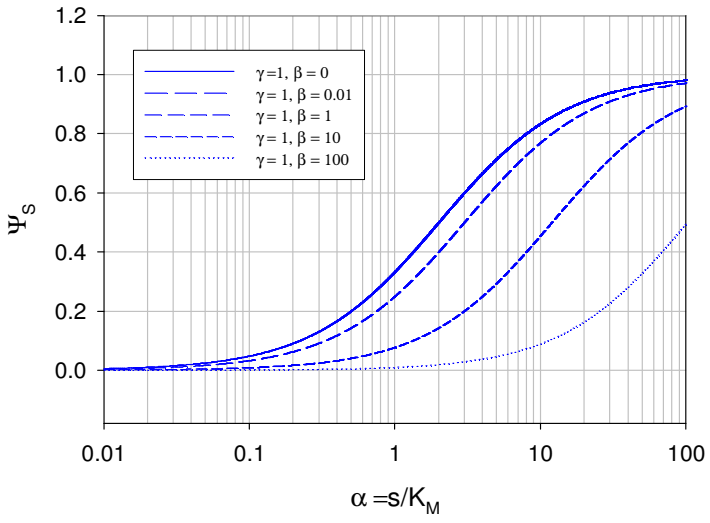

Figure 5. Variation of normalised substrate reaction flux with substrate saturation parameter. The curves are calculated using eqn.23. Here the kinetic competition parameter γ is reasonably small and set at unity. This implies that the flux for reaction between substrate and oxidized enzyme is equal to the flux for reaction between oxidized mediator and reduced enzyme and so neither of the two reactions limit the net rate.

In figure 5 we represent the variation of normalised substrate flux with substrate saturation parameter corresponding to the situation when the kinetic competition parameter $\gamma = 1$. In this circumstance the reaction rate between substrate and oxidized emzyme in the nanotube layer is equal to the reaction flux between oxidized mediator and reduced enzyme. Here the rate of oxidized enzyme regeneration is in balance with the rate of oxidized enzyme loss.

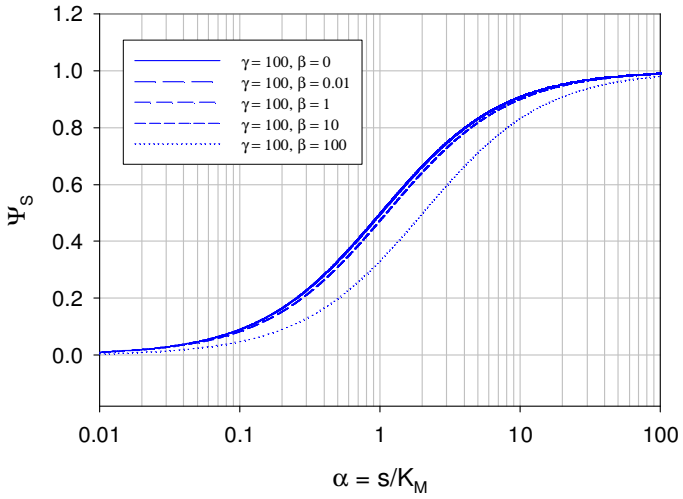

Figure 6. Variation of normalised substrate reaction flux with substrate saturation parameter. The curves are calculated using eqn.23. Here the kinetic competition parameter γ is large and set at 100. This implies that the flux for reaction between substrate and oxidized enzyme is much less than the flux for reaction between oxidized mediator and reduced enzyme and so the former reaction is rate determining.

We note from figure 5 that the substrate reaction flux varies significantly with increasing substrate concentration . The flux levels off when the saturation parameter α is large. Furthermore the shape of the normalised response curve is strongly effected by the numerical value adopted by the mediator saturation parameter β as indeed it should if the reaction kinetics are controlled jointly by the mediator/enzyme and enzyme/substrate reactions. It is interesting to note that the dynamic range of the biosensor depends on the mediator saturation parameter and perhaps the best dynamic range and sensitivity is obtained when the reaction between mediator and enzyme is rate limiting.

In figure 6 we represent the variation of normalised substrate flux with substrate saturation parameter corresponding to the situation when the kinetic competition parameter $\gamma >> 1$. In this case the reaction between substrate and oxidized enzyme is rate limiting and so we note that the curves computed for varying values of the mediator saturation parameter β in the range $0 < \beta < 100$ do not vary much in shape. Again the saturation kinetics are evvident at high substrate concentrations as expected by rate determining Michaelis-Menten enzyme/substrate reaction kinetics.

3. CONCLUSIONS

In this paper we have considered the transport and kinetics of substrate and redox mediator at an assembly of enzymes immobilized within a carbon nanotube mesh dispersed as a thin film on a support electrode surface. We have assumed that the immobilized enzyme layer is thin enough such that diffusion of mediator and substrate within the layer can be neglected. In doing so we have developed simple analytical expressions which serve to quantify the substrate reaction flux and we have related these expressions to the actual flux measured at the support electrode. The balance between mediator and substrate reaction at the enzyme is characterized using a kinetic case diagram.

It should be noted that substrate and mediator diffusive transport within the nanotube film cannot be neglected when the latter is of significant thickness. Under these circumstances the pertinent reaction-diffusion equations for substrate and mediator within the layer must be formulated and solved. This can most readily be accomplished by adapting and extending a methodology previously published by Lyons and co-workers [30] and Bartlett and Whitaker [20]. This analysis will be presented in a subsequent paper.

ACKNOWLEDGEMETNS
MEGL is grateful for the financial support of Enterprise Ireland, Grant Number SC/2003/0049, IRCSET Grant Number SC/2002/0169 and the HEA-PRTLI Programme. The author also wishes to thank Professor P.N. Bartlett, University of Southampton for useful discussion.

Appendix A

In this appendix we outline a derivation of the expression presented in eqn.5 which relates the substrate reaction flux within the layer to the observed flux measured at the underlying support electrode. We have previously noted that the latter quantities are not identical, since some reduced mediator can diffuse through the enzyme layer away from the electrode and be lost into the adjacent solution. To take this fact into account we have written that $f_\Sigma = \eta f_S$. We now will determine an expression for the parameter η following an argument initially proposed by Bartlett and co-workers [19].

Within the enzyme layer we note that the reduced mediator species B (e.g. H_2O_2) is generated at a uniform rate given by the expression f_S/L. Furthermore B is lost from the layer via diffusion away from the support electrode towards the outer edge of the SWNT layer. This process is described by the Fick diffusion equation, and noting that in the steady state the rate of reduced mediator diffusion and generation must balance we can write

$$D_B \frac{d^2 b}{dx^2} + \frac{f_S}{L} = 0 \qquad \text{(A1)}$$

where D_B denotes the diffusion coefficient of B in the enzyme layer and b represents the distance dependent concentration of mediator species within the layer of thickness L. We can consider two boundary conditions:

$$x=0 \quad b=b_0 \quad \left(\frac{db}{dx}\right)_0 = \frac{f_\Sigma}{D_B} = k'b_0 \qquad \text{(A2)}$$
$$x=L \quad b=b_L$$

The boundary condition at x = 0 corresponds to the situation at the support electrode/enzyme layer interface. The first statement is that the potential of the electrode is set to a value such that the concentration of reduced mediator will be set at a defined value b_0. The second statement refers to the fact that the observed flux arises from the oxidation of the reduced mediator at the support electrode surface and that the rate of this process is defined by the heterogeneous rate constant rate constant k' as defined by the Butler-Volmer equation as noted in eqn.2 in the text. The second boundary condition refers to the interface between the enzyme layer and the adjacent solution phase at x = L. Here the reduced mediator concentration has a value b_L .

We integrate eqn.A1 between 0 and L to obtain:

$$D_B\left\{\left(\frac{db}{dx}\right)_L - \left(\frac{db}{dx}\right)_0\right\} = -f_S \qquad \text{(A3)}$$

Noting from eqn.A2 that

$$f_\Sigma = D_B\left(\frac{db}{dx}\right)_0 \qquad \text{(A4)}$$

We obtain

$$D_B\left(\frac{db}{dx}\right)_L = -f_S + f_\Sigma \qquad \text{(A5)}$$

Now the flux of reduced mediator B across the enzyme layer/solution interface can be equated with the diffusive flux of B across the diffusion layer in solution and we note that:

$$D_B\left(\frac{db}{dx}\right)_L = -f_S + f_\Sigma = -\frac{D'_B}{\delta} b_L^* \qquad \text{(A6)}$$

where D'_B denotes the diffusion coefficient of reduced mediator in solution, b^*_L represents the mediator concentration in the solution phase just outside the nanotube layer and δ denotes the Nernst diffusion layer thickness [26]. The latter concentration term is related to the mediator concentration

within the nanotube layer at x = L by $b_L = \kappa_B b_L^*$, where κ_B is the partition coefficient of reduced mediator.

An indefinite integration of eqn.A1 from 0 to x yields

$$\frac{db}{dx} = \frac{f_\Sigma}{D_B} - \frac{f_S}{D_B L} x \tag{A7}$$

Whereas a second integration affords

$$\begin{aligned} b(x) &= b_0 + \frac{f_\Sigma}{D_B} x - \frac{f_S}{2D_B L} x^2 \\ &= \frac{f_\Sigma}{k'} + \frac{f_\Sigma}{D_B} x - \frac{f_S}{2D_B L} x^2 \end{aligned} \tag{A8}$$

When x = L we get $b = b_L$ and so eqn.A8 reduces to

$$b_L = f_\Sigma \left\{ \frac{1}{k'} + \frac{1}{D_B/L} \right\} - \frac{f_S L}{2D_B} \tag{A9}$$

We also note from eqn.A5 that:

$$-\frac{D'_B}{\kappa_B \delta} b_L = -f_S + f_\Sigma \tag{A10}$$

And taking eqn.A9 into consideration we can write:

$$-\frac{D'_B}{\kappa_B \delta} \left\{ f_\Sigma \left(\frac{1}{k'} + \frac{1}{D_B/L} \right) - \frac{f_S L}{2D_B} \right\} = -f_S + f_\Sigma \tag{A11}$$

After some rearrangement we can readily show that

$$f_\Sigma = f_S \left\{ \frac{1 + \frac{1}{2} \frac{D'_B/\delta}{\kappa_B D_B/L}}{1 + \frac{(D'_B/\delta)(D_B/L)}{\kappa_B D_B/L} \left(\frac{1}{k'} + \frac{1}{D_B/L} \right)} \right\} \tag{A12}$$

We can introduce the diffusive flux ratio θ as:

$$\theta = \frac{k'_D}{k_D} = \frac{D'_B/\delta}{\kappa_B D_B/L} \tag{A13}$$

To obtain

$$f_\Sigma = f_S\left\{\frac{1+\frac{\theta}{2}}{1+\theta\left(1+\frac{\kappa_B D_B/L}{\kappa_B k'}\right)}\right\} = f_S\left\{\frac{1+\frac{\theta}{2}}{1+\theta(1+\phi)}\right\} \qquad \text{(A14)}$$

where we have introduced the competition parameter ϕ as

$$\phi = \frac{\kappa_B D_B/L}{\kappa_B k'} \qquad \text{(A15)}$$

This parameter compares the rate of reduced mediator diffusion in the layer to the rate of reduced mediator oxidation at the support electrode surface. Eqn.5 in the main text follows directly from eqn.A14. A plot of the resulting efficiency factor η defined in eqn.5 for various values of the competition parameter ϕ is illustrated in figure A1.

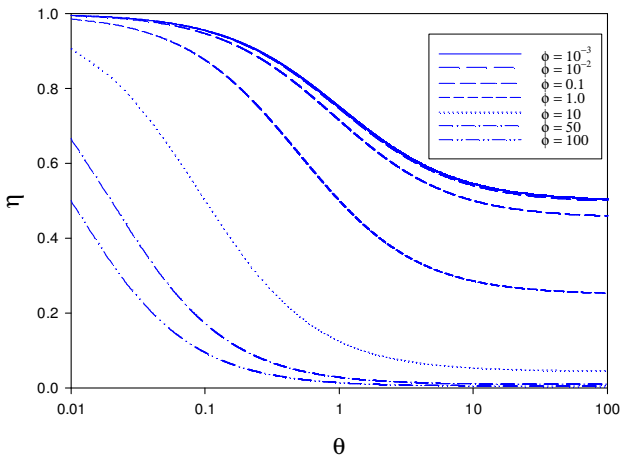

Figure A1. Plot of efficiency factor η defined in eqn.5 of the main text as a function of the normalised parameters θ and ϕ.

Appendix B

In this appendix a derivation of the expression presented in eqn.9 which relates the substrate reaction flux within the layer to the observed flux difference Δf_Σ measured at the underlying support electrode is outlined. The latter quantity is simply the difference in flux for the reduction of the oxidized mediator species A (e.g. O_2) at the support electrode surface which is recorded both in the absence of and in the presence of substrate. In short it defines the flux difference for the 'no substrate' and 'substrate present' situations.

We proceed via an analysis similar to that presented in Appendix A. The net reaction flux for the reduction of the oxidized mediator A is given by the following expression:

$$f_{\Sigma} = D_A \left(\frac{da}{dx} \right)_0 = k' a_0 \qquad \text{(B1)}$$

where a_0 denotes the concentration of oxidized mediator at the support electrode surface. If we let $f_{\Sigma,0}$ denote the reduction flux for oxidized mediator at the electrode surface in the absence of any substrate/enzyme reaction then the flux difference is related to the reaction flux in the layer and is given by eqn.8 in the main text:

$$\Delta f_{\Sigma} = f_{\Sigma,0} - f_{\Sigma} = \eta f_S \qquad \text{(B2)}$$

We need to examine the balance between the diffusion of mediator A to the electrode surface where it will be detected directly, and the reaction of A with the reduced enzyme in the nanotube layer where it will be depleted. We therefore note that

$$D_A \frac{d^2 a}{dx^2} - \frac{f_S}{L} = 0 \qquad \text{(B3)}$$

and the relevant boundary conditions are:

$$\begin{aligned} &x = 0 \quad D_A \left(\frac{da}{dx} \right)_0 = k' a_0 = f_{\Sigma} \\ &x = L \quad a = a_L \end{aligned} \qquad \text{(B4)}$$

It is important to note that [31] in general the reaction flux f_S in eqn.(B3) can be a function of the oxidized mediator concentration a. For f_S to be independent of the oxidized mediator concentration a requires that $k_M a >> k_E s$. This immediately suggests that the response of the biosensor device with respect to glucose will depend greatly on the magnitude of the detection potential applied to the electrode. If the electrode kinetics for oxygen reduction are driven hard then the concentration of A at the electrode surface, $a_0 \to 0$, ($a_0 = f_S / k'$) very quickly and one would not obtain much of a response to added substrate because the concentration of O_2 near the electrode is too low due to electrochemical depletion. Therefore at best we might expect a limited range of response to glucose before the sensor response became oxygen limited. On the other hand if one operates at a detection potential below the limiting current for oxygen reduction, although there might well be a response to glucose, it would possibly not represent the optimum analytical strategy, because any changes in electrode kinetics due to poisoning would have a large effect on the calibration curve.

As before in appendix A we let D_A denote the diffusion coefficient of the oxidized mediator species in the film and set D'_A to be the corresponding oxidized mediator diffusion coefficient in solution with $D'_A = \kappa_A D_A$ and just outside the film we note that $a^*_L = a_L / \kappa_A$ .Integrating eqn.B3 we obtain:

$$D_A \left(\frac{da}{dx} \right)_L - f_{\Sigma} = f_S \qquad \text{(B5)}$$

where we have used the first statement in eqn.B1 to simplify. Now eqn.B5 may be equated with the flux of oxidized mediator A across the diffusion layer

$$D_A\left(\frac{da}{dx}\right)_L = f_\Sigma + f_S = \frac{D'_A}{\delta}\left(a^\infty - a^*{}_L\right) \tag{B6}$$

where a^∞ represents the concentration of oxidized mediator in the bulk solution. This expression may be recast as:

$$f_\Sigma + f_S = \frac{D'_A a^\infty}{\delta} - \frac{D'_A}{\kappa_A \delta} a_L \tag{B7}$$

and we need to derive an expression for a_L. We perform an indefinite integration of eqn.B3 to obtain:

$$\frac{da}{dx} = \frac{f_\Sigma}{D_A} + \frac{f_S}{LD_A}x \tag{B8}$$

A second indefinite integration of eqn.B8 produces

$$a(x) = a_0 + \frac{f_\Sigma}{D_A}x + \frac{f_S}{2LD_A}x^2 \tag{B9}$$

When x = L and noting that $a_0 = f_\Sigma / k'$ we can show that:

$$a_L = \frac{f_\Sigma}{k'} + \frac{f_\Sigma L}{D_A} + \frac{f_S L}{2D_A} \tag{B10}$$

and we have found our expression for a_L. Substituting the latter into eqn.B7 and simplifying we get:

$$f_\Sigma\left\{1 + \frac{D'_A}{\kappa_A \delta}\left(\frac{1}{k'} + \frac{1}{D_A/L}\right)\right\} = \frac{D'_A}{\delta} - f_S\left\{1 + \frac{D'_A L}{2\delta\kappa_A\delta}\right\} \tag{B11}$$

We can readily show that the latter expression reduces to:

$$f_\Sigma = \frac{\frac{D'_A a^\infty}{\delta} - \left(1 + \frac{D'_A L}{2\kappa_A D_A \delta}\right) f_S}{1 + \frac{D'_A}{\kappa_A \delta}\left(\frac{1}{k'} + \frac{1}{D_A/L}\right)} \tag{B12}$$

Eqn.B12 can be simplified still further by multiplying above and below by the factor $\delta / D'_A a^\infty$ to obtain

$$f_{\Sigma} = \frac{1 - \frac{1}{D'a^{\infty}/\delta}\left(1 + \frac{D'_A L}{2\kappa_A D_A \delta}\right) f_S}{\frac{1}{D'a^{\infty}/\delta} + \frac{1}{\kappa_A k'a^{\infty}} + \frac{1}{\kappa_A D_A a^{\infty}/L}} \tag{B13}$$

Now when we 'turn off' the enzyme reaction we only consider the direct reduction of oxidized mediator at the support electrode surface and we set $f_S = 0$ in eqn.B13 to obtain:

$$f_{\Sigma,0} = \frac{1}{\frac{1}{D'_A a^{\infty}/\delta} + \frac{1}{\kappa_A k'a^{\infty}} + \frac{1}{\kappa_A D_A a^{\infty}/L}} \tag{B14}$$

It is very gratifying to note from eqn.B13 that the presence of the substrate reaction *reduces* the value of the observed mediator reduction flux via the participation of the f_S term. Hence one expects that the amperometric response should *decrease* (when compared with the response recorded in the absence of substrate) with *increasing* substrate concentration. This is because there is less oxidized mediator available for direct electrode reaction as the concentration of substratr increases ddue to the increased quantity of reduced enzyme produced in the catalytic reaction which must be reacted with. The experimental data underpinning the latter observation was recently reported by the author and confirmed by others [16,32].

We note that in the absence of added substrate the oxidized mediator reduction flux consists of three distinct terms : the diffusive flux of oxidized mediator in the nernst diffusion layer, the diffusive flux of oxidized mediator within the nanotube layer and the heterogeneous electron transfer kinetics of the oxidized mediator reduction at the support electrode surface. We can simplify the notation by introducing the following definitions:

$$f'_D = \frac{D'_A a^{\infty}}{\delta} \quad f_D = \frac{D_A a^{\infty}}{L} \quad f_K = \kappa_A k'a^{\infty} \tag{B15}$$

Hence eqn.B13 reduces to:

$$f_{\Sigma} = \frac{1 - \frac{1}{f'_D}\left(1 + \frac{f'_D}{2f_D}\right) f_S}{\frac{1}{f'_D} + \frac{1}{f_K} + \frac{1}{f_D}} \tag{B16}$$

Whereas eqn.B14 reduces to:

$$f_{\Sigma,0} = \frac{1}{\frac{1}{f'_D} + \frac{1}{f_K} + \frac{1}{f_D}} \tag{B17}$$

We define the flux difference as:

$$\Delta f = f_{\Sigma,0} - f_{\Sigma} = \frac{\frac{1}{f'_D} + \frac{1}{2f_D}}{\frac{1}{f'_D} + \frac{1}{f_D} + \frac{1}{f_K}} f_s = \frac{1 + \frac{f'_D}{2f_D}}{1 + \frac{f'_D}{f_D} + \frac{f'_D}{f_K}} f_S \tag{B18}$$

Again introducing an efficiency factor η' as:

$$\eta' = \frac{1 + \frac{f'_D}{2f_D}}{1 + \frac{f'_D}{f_D} + \frac{f'_D}{f_K}} = \frac{1 + \frac{\theta}{2}}{1 + \theta + \varepsilon} \tag{B19}$$

Where we define:

$$\theta = \frac{f'_D}{f_D} \quad \varepsilon = \frac{f'_D}{f_K} \tag{B20}$$

And we have derived eqn.9 of the main text.

References

1. (a) N.L. Rosi, C.A. Mirkin, *Chem. Rev*., 105(2005) 1547 ; (b) M. Keusgen, *Naturwissenschaften*, 89(2002) 433 ; (c) J.C. Love, L.A. Estroff, J.K. Kriebel, R.G. Nuzzo, G.M. Whitesides, *Chem. Rev.,* 105(2005) 1103.
2. S. Iijima , *Nature* , 354(1991) 56.
3. (a) J.J. Gooding, *Electrochim. Acta* 50 (2005) 3049 ; (b) C.N.R. Rao, B.C. Satishkurnar, A. Govindaraj, M. Nath, *ChemPhysChem.*, 2(2001) 78.
4. J.Wang, *Electroanalysis*, 17(2005) 7.
5. E. Katz, I. Willner, *ChemPhysChem*., 5(2004) 1084.
6. A.M. Kuznetsov, J. Ulstrup, *Electron transfer in chemistry and biology*, 1998, Wiley, New York.
7. (a) I. Willner, B. Willner, E. Katz, *Rev. Mol. Biotech*.,82(2002) 325 ; (b) F.A. Armstrong, *Curr. Opin. Chem. Biol.* 9(2005) 110.
8. (a) I. Willner, B. Willner, *Trends in Biotechnology*, 19(2001) 222 ; (b) I. Willner, E. Katz, *Angew. Chem. Int. Ed.*, 39(2000) 1180.
9. K. Habermuller, M. Mosbach, W. Schuhmann, *Fresenius J Anal Chem.*, 366(2000) 560.
10. W. Schuhmann, *Rev. Mol. Biotechnol*., 82(2002) 425.
11. (a) J.J. Gooding, *Electrochim. Acta*, 50(2005) 3049 ; (b) J. Wang, *Electroanalysis*, 17(2005) 7 ; (c) E. Katz, I. Willner, *ChemPhysChem.* 5(2004) 1084.
12. (a) A. Guiseppi-Elie, C. Lei, R.H. Baughman, *Nanotechnology*, 13(2002) 559 ; (b) C. Cai, J. Chen, *Anal. Biochem*., 332(2004) 75.
13. (a) W. Liang, Y. Zhuobin, *Sensors*, 3(2003) 544 ; (b) M. Wang, Y. Shen, Y. Liu, T. Wang, F. Zhao, B. Liu, S. Dong, *J. Electroanal. Chem.,* 578(2005) 121; (c) Y. Yin, Y. Lu, P. Wu, C. Cai, *Sensors*, 5(2005) 220.
14. G. Wang, J.J. Xu, H.Y. Chen, *Electrochem. Commun.*, 4(2002) 506.
15. (a) J. Wang, M. Musameh, *Anal. Chem*., 75(2003) 2075 ; (b) J.J. Gooding, R. Wibowo, J. Liu, W. Yang, D. Losie, S. Orbons, F.J. Mearns, J.G. Shapter, D.B. Hybbert, *J. Am. Chem. Soc*., 125(2003)

9006 ; (c) J. Liu, A. Chou, W. Rahmat, M.N. Paddon-Row, J.J. Gooding, *Electroanalysis*, 17(2005) 38.
16. M.E.G. Lyons and G.P. Keeley, *Chem. Commun.*, (2008) 2529.
17. M.E.G. Lyons and G.P. Keeley, *Sensors*, 6(2006) 1791.
18. M.E.G. Lyons and G.P. Keeley, *Int. J. Electrochem. Sci.,* 3(2008)819.
19. P.N. Bartlett, P. Tebbutt, C.H. Tyrrell, *Anal. Chem.*, 64(1992) 138.
20. M.E.G. Lyons, *Sensors*, 3(2003) 19.
21. (a) P.N. Bartlett and R.G. Whitaker, *J. Electroanal. Chem.*, 224(1987) 27; (b) P.N. Bartlett and R.G. Whitaker, *J. Electroanal. Chem.*, 224(1987) 37.
22. M. Marchesiello and E. Genies, *J. Electroanal. Chem.*, 358(1993) 35.
23. P.N. Bartlett and K.F.E. Pratt, *J. Electroanal. Chem.*, 397(1995) 61.
24. M.E.G. Lyons in *Electroactive Polymer Electrochemistry : Part 1 Fundamentals.* M.E.G. Lyons (Ed), Plenum Press, New York, 1994, pp. 237-374.
25. P.N. Bartlett, C.S. Toh, E.J. Calvo and V. Flexer, *Bioelectrochemistry: Fundamentals, Experimental Techniques and Applications*. P.N. Bartlett (Ed). Wiley, New York, 2008, Chapter 8.
26. W.J. Albery, *Electrode Kinetics,* Clarendon Press, Oxford, 1975. Chapter 3.
27. M.E.G. Lyons, *Sensors*, 1(2001) 215.
28. M.E.G. Lyons, Sensors, 2(2002) 473.
29. M.E.G. Lyons, C.H. Lyons, A. Michas, P.N. Bartlett, *J. Electroanal. Chem.*, 351(1993) 245.
30. M.E.G. Lyons, J.C. Greer, C.A. Fitzgerald, T. Bannon and P.N. Bartlett, *Analyst*, 121(1996)715.
31. P.N. Bartlett, personal communication, 2008.
32. M.M. Rahman, A. Umar, K. Sawada, *Sensors & Actuators B*, in press.